A family of mixed-valent Mn^{IV}Mn$_6^{III}$Mn$_6^{II}$ tridecanuclear clusters, and their magnetostructural correlation

Christos Lampropoulos, Muralee Murugesu, Khalil A. Abboud, George Christou *

Department of Chemistry, University of Florida, Gainesville, FL 32611-7200, USA

Abstract

Three tridecanuclear Mn complexes [Mn$_{13}$O$_8$(OH)$_6$(ndc)$_6$] · 8DMF · H$_2$O (**1**), [Mn$_{13}$O$_8$(EtO)$_{5.5}$(OH)$_{0.5}$(ndc)$_6$] · 6MeCN · 2H$_2$O (**2**), and [Mn$_{13}$O$_8$(EtO)$_6$(O$_2$CPh)$_{12}$] · 7H$_2$O (**3**) (ndc^{2-} = 1,8-naphthalenedicarboxylate) are reported. Complexes **1–3** possess a central core comprised of three layers: The middle layer is a central Mn^{IV} atom surrounded by a planar ring of six Mn^{II} atoms, and above and below this are two Mn$_3^{III}$ triangular units. Complexes **1** and **2** represent the first use of ndc^{2-} in manganese chemistry. All three complexes are mixed-valent Mn^{IV}Mn$_6^{III}$Mn$_6^{II}$. Complex **1** was found to have a ground state spin of $S = 9/2$, whereas **2** and **3** have $S = 11/2$ despite the nearly isostructural core of the three compounds. A magnetostructural correlation has shown that small structural perturbations can considerably change the magnetic properties of these clusters.
© 2006 Elsevier Ltd. All rights reserved.

Keywords: Manganese; 1,8-Naphthalenedicarboxylate; Polynuclear metal complexes; Magnetic properties; Magnetostructural correlation

Polynuclear manganese clusters have been the main source over the last several years of high-spin species, many of which behave as single-molecule magnets (SMMs). SMMs are molecular complexes that behave as molecular superparamagnets and thus as nanoscale magnetic particles (nanomagnets). These molecules combine a large spin ground state with a relatively large and negative magnetoanisotropy of the easy-axis or Ising-type (negative zero-field splitting parameter, D), resulting in the observation of hysteresis in magnetization versus applied field studies [1]. Such nanoscale materials also straddle the classical/quantum interface, displaying not just the classical property of magnetization hysteresis but also the quantum properties of quantum tunneling of the magnetization (QTM) through the anisotropy barrier [2], and quantum phase interference [3]. That manganese complexes are the main source of SMMs is consistent with their propensity to display unusually large ground state spins and large D

values, the latter arising from the presence of Jahn–Teller distorted Mn^{III} ions. One of the few ways to gain an understanding of the various factors influencing the exchange interactions between the metal centers and thus the ground state spin values is through a magnetostructural correlation between structurally similar systems differing in core structural parameters. However, this is not a trivial task since the synthesis of structurally related complexes and thus families of clusters with non-identical ground state S values is extremely challenging.

A variety of ligands have been employed over the years in the search for new magnetically interesting clusters, with monocarboxylates being a very common type. In contrast, dicarboxylates have not been as extensively used, even though they are attractive on paper as a route to polynuclear products as a result of their bifunctional nature. We have previously reported various complexes that employ dicarboxylates [4] and have recently extended this work to less flexible varieties. One example of a dicarboxylic acid with reduced flexibility is 1,8-naphthalenedicarboxylic acid (ndcH$_2$) in which the two carboxylate groups are nearly

---

parallel. This group has not previously been used in manganese chemistry, but we have found that it yields interesting products. We herein report two mixed-valent (Mn_6^{II}, Mn_6^{III}, Mn^{IV}) tridecanuclear Mn clusters obtained using the ndc^{2-} ligand. In addition, a route has been found to an analogous Mn_{13} species with only monocarboxylate groups. The magnetic properties vary significantly within this family, and a qualitative magnetostructural correlation has provided some insight into the influence on the observed properties of the mono- versus dicarboxylate ligation.

The reaction of $Mn(O_2CMe)_2 \cdot 4H_2O$ in DMF with 1,8-naphthalic anhydride and NEt_3 led to subsequent isolation, on layering with Et_2O, of $[Mn_{13}O_8(OH)_6(ndc)_6] \cdot 8DMF \cdot H_2O$ (1) in ∼70% yield. When the same reaction solution was layered with EtOH, the product was $[Mn_{13}O_8(EtO)_{5.5}(OH)_{0.5}(ndc)_6] \cdot 6MeCN \cdot 2H_2O$ (2) in similar yield. Finally, reaction of preformed $[Mn_3O(O_2CPh)_6(pyr)_2(H_2O)]$ [5] with NEt_3 in EtOH produced $[Mn_{13}O_8(EtO)_6(O_2CPh)_{12}] \cdot 7H_2O$ (3) in ∼80% yield. Fuller details of the syntheses will be provided in the full paper [6].

Complex **1** crystallizes in the triclinic space group $P\bar{1}$ with the molecule on an inversion center. The core of the cluster (Fig. 1) contains one Mn^{IV}, six Mn^{II}, and six Mn^{III} ions held together by six μ_5-O^{2-}, two μ_3-O^{2-}, and six μ_3-OH^- ions. Peripheral ligation is provided by six ndc^{2-} groups whose carboxylate arms each bridge two Mn atoms. The only Mn^{IV} atom (Mn6) is located at the center of the cluster, surrounded by a nearly planar ring of six Mn^{II} atoms (Mn3, Mn4, Mn7, and their symmetry equivalents). The six Mn^{III} atoms (Mn1, Mn2, Mn5, and their symmetry equivalents) form two equilateral triangles, one above and one below the nearly planar Mn_6^{II} ring. The OH^- groups are O atoms O14, O15, O17, and their symmetry partners. Alternatively, the $[Mn_{13}O_{14}]$ core can be described as eight face-fused $[Mn_4O_4]$ cubane units with a common vertex at the central Mn^{IV} atom (Mn6). Each cubane shares three of

its faces with its neighbors, creating a larger cubane-like unit whose eight vertices are all O atoms; in this description, the Mn atoms each lie at the mid-point of an edge and at the center of the larger cubane. The thirteen Mn ions in **1** are all six-coordinate with near-octahedral geometry, and their assigned oxidation states were established by charge considerations, bond valence sum calculations [6], and the clear Jahn–Teller (JT) distortions (elongations) at the Mn^{III} ions.

Complex **2** crystallizes in the triclinic space group $P\bar{1}$. The core of the cluster again contains one Mn^{IV}, six Mn^{II}, and six Mn^{III} ions, but now held together by six μ_5-O^{2-}, two μ_3-O^{2-}, and six μ_3-OEt^- ions. Thus, the six OH^- groups in **1** are EtO^- groups in **2**; however, one EtO^- group is disordered with a OH^- group, with ∼50:50 relative occupancies. Peripheral ligation is again by six ndc^{2-} groups. Complex **2** is thus structurally very similar to **1**, with small differences as summarized in Table 1.

Complex **3** crystallizes in the monoclinic space group $C2/c$. The core of the cluster again contains one Mn^{IV}, six Mn^{II}, and six Mn^{III} ions, held together as in **2** by six μ_5-O^{2-}, two μ_3-O^{2-}, and six μ_3-OEt^- ions (with no disorder in the occupancies of the latter). However, the peripheral ligation is now provided by 12 benzoate groups, each bridging two Mn atoms (Fig. 2). The core is thus very similar with those of **1** and **2**, with various small differences as summarized in Table 1. Note that complex **3** has also been previously obtained by others from a very different procedure [7].

The cores of the structures of **1–3** are thus overall very similar to each other, except for the OH^- versus EtO^- difference (Figs. 1–3). Closer inspection of the structures and the metric parameters in Table 1 reveal few major differences. The biggest, of course, is the $C \cdots C$ separation between two adjacent carboxylate groups. In **1** and **2**, this is only 2.899 ± 0.042 and 2.909 ± 0.017 Å, respectively, since the two carboxylate groups are attached to the
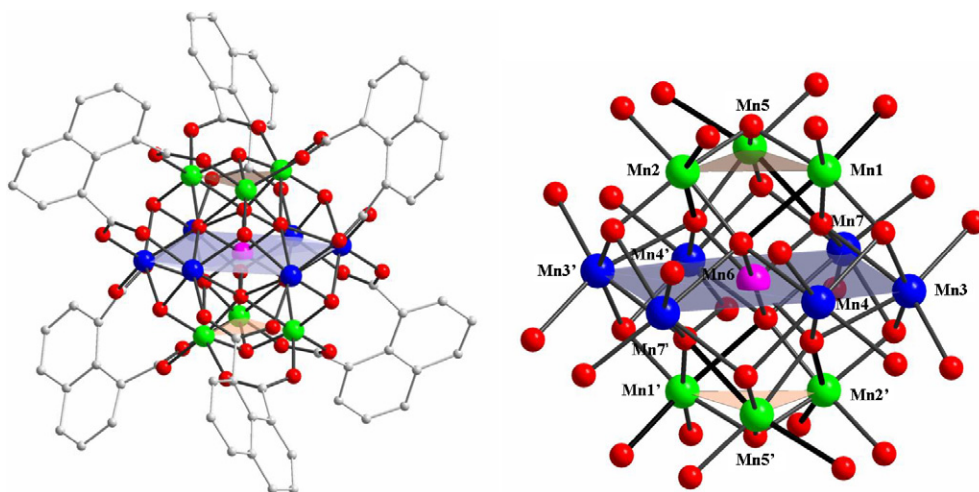

Fig. 1. The structure of complex **1** (left) and its partially labeled core (right). Color code: Mn^{II} blue, Mn^{III} green, Mn^{IV} purple, O red, C grey. (For interpretation of the references in color in this figure legend, the reader is referred to the web version of this article.)

Table 1
Structural comparisons between complexes **1**, **2**, and **3**

Parameter[a]	1	2	3
$C \cdots C$ (Å)	2.899 ± 0.042	2.909 ± 0.017	3.434 ± 0.043
$Mn^{III} \cdots Mn^{III}$ (Å)	2.945 ± 0.004	2.987 ± 0.010	2.952 ± 0.003
$Mn^{II} \cdots Mn^{III}$ (Å)	3.186 ± 0.013	3.177 ± 0.038	3.202 ± 0.043
$Mn^{II} \cdots Mn^{IV}$ (Å)	3.239 ± 0.021	3.195 ± 0.007	3.206 ± 0.008
$Mn^{II} \cdots Mn^{II}$ (Å)	3.250 ± 0.031	3.208 ± 0.041	3.207 ± 0.020
$Mn^{III} \cdots Mn^{IV}$ (Å)	3.018 ± 0.008	3.054 ± 0.010	3.061 ± 0.008
$Mn^{III}-\mu_5O^{2-}-Mn^{III}$ (°)	86.17 ± 0.18	86.43 ± 0.19	84.35 ± 0.35
$Mn^{III}-\mu_3O^{2-}-Mn^{III}$ (°)	103.85 ± 0.75	102.25 ± 0.45	104.20 ± 0.40
$Mn^{II}-O^{2-}-Mn^{IV}$ (°)	99.93 ± 1.08	98.54 ± 1.30	98.85 ± 2.75
$Mn^{III}-O^{2-}-Mn^{IV}$ (°)	97.16 ± 6.94	97.42 ± 6.78	97.40 ± 7.80
$Mn^{II}-O^{2-}-Mn^{II}$ (°)	88.18 ± 0.53	88.15 ± 1.70	88.41 ± 0.50
trans $Mn^{II}-\mu_5\text{-}O^{2-}-Mn^{III}$ (°)	162.15 ± 7.65	162.60 ± 7.90	161.85 ± 6.55
cis $Mn^{II}-\mu_5O^{2-}-Mn^{III}$ (°)	90.66 ± 5.03	90.41 ± 5.20	91.55 ± 6.65
$Mn^{II}-RO^{-}-Mn^{III}$ (°)	102.30 ± 1.60	101.11 ± 1.26	100.80 ± 1.60
$Mn^{II}-RO^{-}-Mn^{II}$ (°)	96.49 ± 0.02	94.66 ± 0.54	92.30 ± 0.30
$O^{2-} \cdots Mn_3^{III}$ plane (Å)	0.782	0.837	0.769
$Mn^{IV} \cdots Mn_3^{III}$ plane (Å)	2.492	2.520	2.543

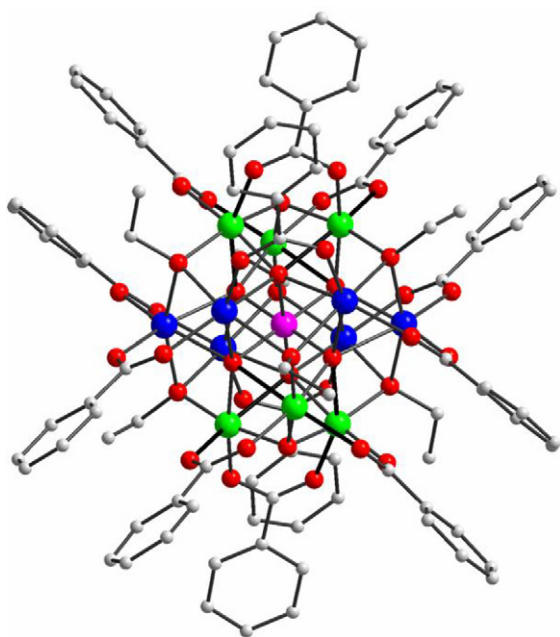[a] Average values; indicated are the ranges in that parameter.

Fig. 2. The structure of complex **3**. Color code: Mn^{II} blue, Mn^{III} green, Mn^{IV} purple, O red, C grey. (For interpretation of the references in color in this figure legend, the reader is referred to the web version of this article.)

naphthalene backbone, and these are much shorter than the 3.434 ± 0.043 Å between two separate benzoate groups in **3**. However, this strain imposed on the disposition of the peripheral carboxylate ligands does not appear to have a significant effect on the distances and angles within the $[Mn_{13}O_{14}]$ core. The metric parameters of benzoate complex **3** are essentially all within the ranges of the corresponding values of either **1** or **2**, or both. In approximately half the entries in Table 1, there are no differences between the three complexes. Among the remainder, it is interesting

to note that for some parameters ($Mn^{III} \cdots Mn^{III}$, $Mn^{II} \cdots Mn^{III}$ distances, and $Mn^{III}-\mu_3\text{-}O^{2-}-Mn^{III}$ angles), the values for **1** are closer to those **3** than those for **2**. This suggests that for many of the metric parameters, changes caused by the HO^{-}-to-EtO^{-} substitution (**1** to **2**) are essentially equal and opposite to those due to the ndc^{2-}-to-$PhCO_2^{-}$ substitution (**2** to **3**), resulting in some parameters for **1** being the same as those for **3**. In other cases, the values for **2** are closest to those for **3** (e.g. $Mn^{II} \cdots Mn^{II}$, $Mn^{II} \cdots Mn^{IV}$, and $Mn^{III} \cdots Mn^{IV}$ distances, $Mn^{II}-O^{2-}-Mn^{IV}$ angles) showing the values are dominated by the EtO^{-} versus OH^{-} difference.

With respect to the magnetic properties to be discussed below, a probably significant difference within Table 1 is found in the $Mn^{II}-RO^{-}-Mn^{II}$ angles, where R = H (**1**) or Et (**2**, **3**). In this case, the values for the latter two are both smaller than that of **1**. This is likely a contributory factor in the observed differences in magnetic properties to be discussed below, because it is well known that even very small changes in the angles at monoatomic bridges between two metal atoms can have a significant effect on the magnitude of the resulting superexchange interaction [8]; this was first demonstrated in the classic work on bis-hydroxo-bridged Cu(II) dimers [9].

Solid state, variable-temperature magnetic susceptibility measurements were performed on vacuum-dried micro-crystalline samples of complexes **1**, **2**, and **3** suspended in eicosane to prevent torquing. The dc magnetic susceptibility (χ_M) data were collected in the 5.0–300 K range in a 0.1 Tesla (T) (1000 Oe) magnetic field. The obtained data are plotted as $\chi_M T$ versus T in Fig. 4, and it can be seen that the overall profiles are very similar for the three complexes, $\chi_M T$ steadily decreasing with decreasing temperature and thus suggesting dominant antiferromagnetic interactions between the metal centers in the molecule. However, the plots for **1** and **3** are the most similar, which
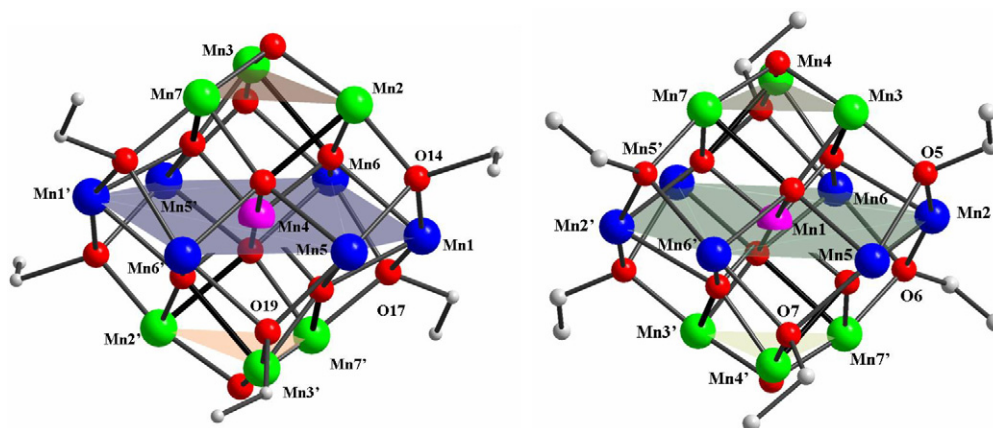
Fig. 3. Partially labeled cores of complexes **2** (left) and **3** (right). Color code: Mn^{II} blue, Mn^{III} green, Mn^{IV} purple, O red, C grey. (For interpretation of the references in color in this figure legend, the reader is referred to the web version of this article.)
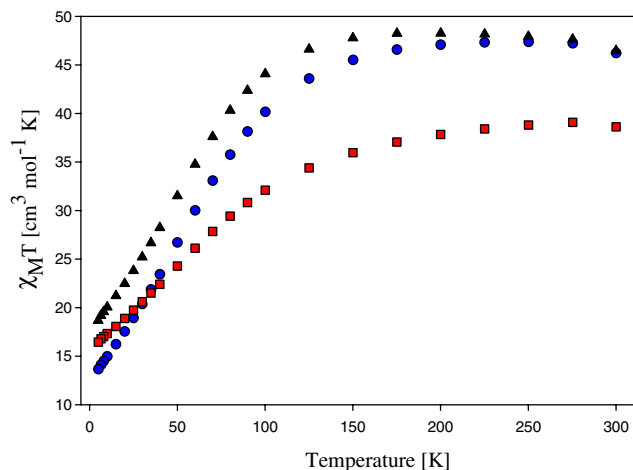

Fig. 4. $\chi_M T$ vs. T for complexes **1** (●), **2** (■), and **3** (▲) in a 0.1 T applied dc field.

likely reflects the fact that these two complexes have several similar core metric parameters, as described above.

For all three compounds, the 5.0 K data suggest that the complexes all possess ground states with significant S values. This would not be unexpected for such a complicated Mn_{13} topology with multiple inequivalent exchange parameters, most of which, if not all, being almost certainly antiferromagnetic. This is because of the spin frustration effects expected within the many Mn_3 triangular units within the Mn_{13} structure. We define spin frustration here in its more general form as competing exchange interactions of comparable magnitude that prevent (frustrate) the preferred pairwise antiparallel spin alignments that would give small (0 or 1/2) ground states.

In order to determine the ground states of complexes **1**, **2**, and **3**, magnetization (M) data were collected in the magnetic field and temperature ranges of 0.1–7 T and 1.8–10 K, respectively. Attempts to fit the resulting data using the program MAGNET [10], which assumes that only the ground state is populated at these temperatures, includes axial zero-field splitting (ZFS) and the Zeeman interaction with

the applied field, and carries out a full powder average, did not lead to satisfactory fits. In our experience, this is the case when there are low-lying excited states that are consequently populated even at these relatively low temperatures and/or excited states that are more separated from the ground state but have S values greater than that of the ground state and thus their larger M_S levels rapidly decrease in energy due to the applied magnetic field and approach (or even cross) those of the ground state. Such situations are expected for **1**–**3** because of their high Mn^{II} content (exchange interactions involving Mn^{II} are known to be very weak and almost always antiferromagnetic, yielding small energy separations between the ground state and many nearby excited states with larger S values), and will lead to poor fits of the magnetization data since the fitting program assumes population of only the ground state levels. As we have described elsewhere on multiple occasions [11], these complications can sometimes be avoided by using only data collected at the lowest fields. For complex **1**, a satisfactory fit was obtained using data collected in the field range 0.1–0.8 T, as shown in Fig. 5, with fit parameters $S = 9/2$, $g = 2.00(1)$ and $D = -0.14(1)$ cm^{-1}. However, attempts to fit the magnetization data for complexes **2** and **3** collected at only the lower fields still did not lead to acceptable fits. Therefore, we turned to the use of more reliable methods based on ac magnetic susceptibility measurements [12], which do not employ a dc field, to identify the ground state spins of **2** and **3**, and also confirm (or otherwise) our initial conclusion of an $S = 9/2$ ground state for **1**.

Alternating-current magnetic susceptibility studies were performed on vacuum-dried microcrystalline samples of **1**–**3** in the temperature range 1.8–15 K in a zero dc field and a 3.5 Oe ac field oscillating at frequencies between 250 and 1000 Hz. The resulting data are plotted as $\chi'_M T$ versus T in Fig. 6, where χ'_M is the in-phase component of the ac susceptibility. For all three complexes, $\chi'_M T$ decreases essentially linearly with decreasing temperature, this downward slope supporting a decreasing population of excited
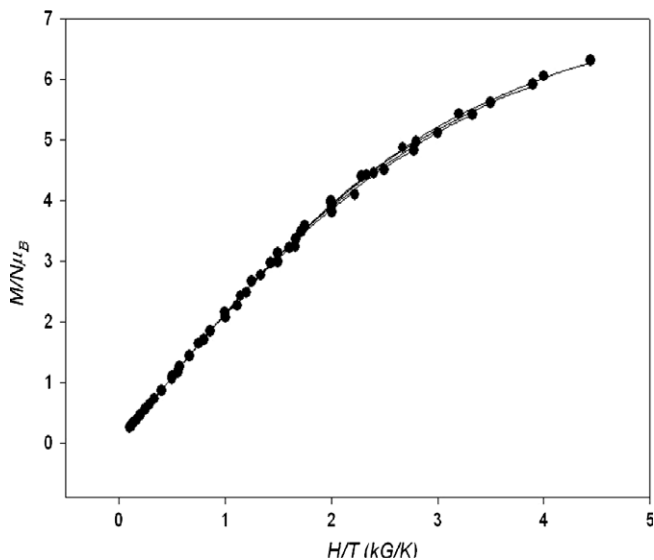
Fig. 5. Plot of the reduced magnetization, $M/N\mu_B$, vs. H/T for complex **1**; the solid line is the fit of the data (see the text for the fitting parameters and the fields used).

states with a larger S than the ground state, in agreement with the statements above re the dc magnetization fitting problems. A linear extrapolation of the data for **1** to 0 K, where only the ground state will be populated, gives an approximate $\chi'_M T$ of ~ 13 cm^3 mol^{-1} K, indicating an $S = 9/2$ ground state (expected spin-only ($g = 2.0$) value for $S = 9/2$ is 12.4 cm^3 mol^{-1} K). This is satisfyingly consistent with the conclusion from the dc magnetization fit in Fig. 5. For complexes **2** and **3**, the $\chi'_M T$ values are significantly higher, and extrapolations to 0 K give approximate values of $\chi'_M T$ of ~ 16.2 and ~ 17 cm^3 mol^{-1} K, respectively, consistent with a $S = 11/2$ ground states for these complexes (spin-only value for $S = 11/2$ is 17.88 cm^3 mol^{-1} K).

It is interesting that complexes **1** and **3** have the overall more similar $\chi_M T$ versus T behavior up to 300 K (Fig. 4)
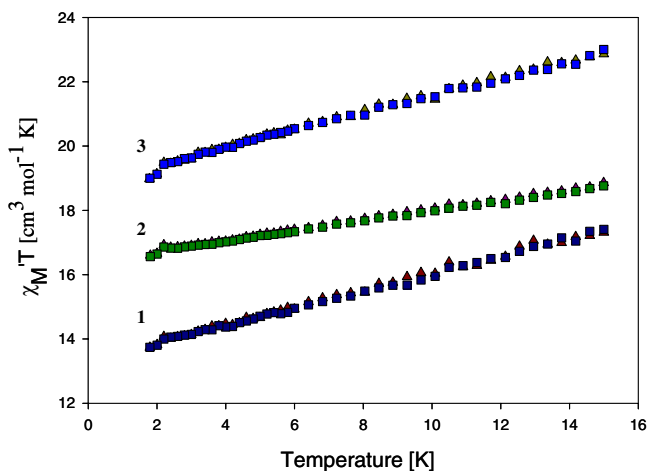
but that **2** and **3** are the more similar at very low temperatures and in their ground states (Figs. 4 and 6). The former observation is consistent with the several structural similarities between **1** and **3** seen in Table 1, even though they differ in both the EtO$^-$ versus OH$^-$ and benzoate versus ndc^{2-} identities, whereas the difference in ground state is perhaps due to the significantly different Mn^{II}Mn^{II} exchange interactions via the Mn^{II}–RO$^-$–Mn^{II} superexchange pathways. These are likely the weakest interactions in the molecule, their impact thus becoming evident only at the lowest temperatures, and given the significant difference in the angles at the bridging HO$^-$ or EtO$^-$ atoms mentioned earlier, it seems reasonable that differences in this exchange parameter could cause a flip in the relative energies of some of the closely separated, lowest-lying spin states, causing a change in the ground state.

In summary, the initial use of the ndc^{2-} group in Mn chemistry has led to two mixed-valent Mn$_{13}$ clusters containing three different oxidation states of this metal and differing only in the HO$^-$ versus EtO$^-$ identity of some of the bridging ligands. In addition, a rational and convenient synthesis has been developed for the corresponding benzoate version, which was already known in the literature. The unusual $\eta^1:\eta^1:\eta^1:\eta^1:\mu_4$ coordination mode adopted by the ndc^{2-} group suggests that it may prove a route to a variety of new metal clusters with other transition metals or lanthanides. Examination of the structural parameters of the three complexes **1**, **2**, and **3** led to the conclusion that the inflexible ndc^{2-} group actually imposes little significant structural change on the core of the molecule, and what is seen appears comparable with the HO$^-$ versus EtO$^-$ effect. Complexes **1**–**3** were determined to have $S = 9/2$, 11/2, and 11/2 ground states, respectively; a fuller rationalization of this difference will be provided in the full report of this work.

Acknowledgement

Appendix A. Supplementary material

CCDC 617346, 617347 and 617348 contain the supplementary crystallographic data for this paper. These data can be obtained free of charge via http://www.ccdc.cam.ac.uk/conts/retrieving.html, or from the Cambridge Crystallographic Data Centre, 12 Union Road, Cambridge CB2 1EZ, UK; fax: (+44) 1223-336-033; or e-mail: deposit @ccdc.cam.ac.uk. Supplementary data associated with this article can be found, in the online version, at doi:10.1016/j.poly.2006.10.038.

Fig. 6. Plot of the in-phase (χ'_M) ac magnetic susceptobility (as $\chi'_M T$) vs. T for complexes **1**, **2**, and **3** in a 3.5 Oe field oscillating at 250 (▲) and 1000 (■) Hz. The blips at 2.2 K are instrumental artifacts.

References

[1] (a) G. Christou, D. Gatteschi, D.N. Hendrickson, R. Sessoli, MRS Bull. 25 (2000) 66;

(b) R. Sessoli, H.-L. Tsai, A.R. Schake, S. Wang, J.B. Vincent, K. Folting, D. Gatteschi, G. Christou, D.N. Hendrickson, J. Am. Chem. Soc. 115 (1993) 1804;
(c) R. Sessoli, D. Gatteschi, A. Caneschi, M.A. Novak, Nature 365 (1993) 141;
(d) G. Christou, Polyhedron 24 (2005) 2065;
(e) W. Wernsdorfer, N. Aliaga-Alcalde, D.N. Hendrickson, G. Christou, Nature 416 (2002) 406;
(f) M. Soler, W. Wernsdorfer, K.A. Abboud, D.N. Hendrickson, G. Christou, Polyhedron 22 (2003) 1777;
(g) M. Soler, W. Wernsdorfer, K.A. Abboud, J.C. Huffman, E.R. Davidson, D.N. Hendrickson, G. Christou, J. Am. Chem. Soc. 125 (2003) 3576;
(h) H. Andres, R. Basler, A.J. Blake, C. Cadiou, G. Chaboussant, C.M. Grant, H.-U. Güdel, M. Murrie, S. Parsons, C. Paulsen, F. Semadini, V. Villar, W. Wernsdorfer, R.E.P. Winpenny, Chem. Eur. J. 8 (2002) 4867;
(i) E.K. Brechin, M. Soler, G. Christou, M. Helliwell, S.J. Teat, W. Wernsdorfer, Chem. Commun. (2003) 1276;
(j) D.J. Price, S.R. Batten, B. Moubaraki, K.S. Murray, Chem. Commun. (2002) 762.
[2] J.R. Friedman, M.P. Sarachik, J. Tejada, R. Ziolo, Phys. Rev. Lett. 76 (1996) 3830.
[3] (a) W. Wernsdorfer, R. Sessoli, Science (2000) 2417;
(b) W. Wernsdorfer, M. Soler, G. Christou, D.N. Hendrickson, J. Appl. Phys. 91 (2002) 7164;
(c) W. Wernsdorfer, N.E. Chakov, G. Christou, Phys. Rev. Lett. 95 (1–4) (2005) 037203.

[4] (a) R.C. Squire, S.M.J. Aubin, K. Folting, W.E. Streib, G. Christou, D.N. Hendrickson, Inorg. Chem. 34 (1995) 6463;
(b) M.W. Wemple, H.L. Tsai, S. Wang, J.P. Claude, W.E. Streib, J.C. Huffman, D.N. Hendrickson, G. Christou, Inorg. Chem. 35 (1996) 6437;
(c) C. Canada-Vilalta, W.E. Streib, J.C. Huffman, T.A. O'Brien, E.R. Davidson, G. Christou, Inorg. Chem. 43 (2004) 101.
[5] J.B. Vincent, H.R. Chang, K. Folting, J.C. Huffman, G. Christou, D.N. Hendrickson, J. Am. Chem. Soc. 109 (1987) 5703.
[6] Details will be given in the full paper.
[7] Z. Sun, P.K. Gantzel, D.N. Hendrickson, Inorg. Chem. 35 (1996) 6640.
[8] O. Kahn, Molecular Magnetism, VCH, New York, 1993.
[9] W.H. Crawford, H.W. Richardson, J.R. Wasson, D.J. Hodgson, W.E. Hartfield, Inorg. Chem. 15 (1976) 2107.
[10] E.R. Davidson, MAGNET, Indiana University, Bloomington, IN, 1999.
[11] (a) M. Soler, W. Wernsdorfer, K. Folting, M. Pink, G. Christou, J. Am. Chem. Soc. 126 (2004) 2156;
(b) E.C. Sanudo, W. Wernsdorfer, K.A. Abboud, G. Christou, Inorg. Chem. 43 (2004) 4137;
(c) M. Murugesu, J. Raftery, W. Wernsdorfer, G. Christou, E.K. Brechin, Inorg. Chem. 43 (2004) 4203.
[12] (a) E.K. Brechin, C. Boskovic, W. Wernsdorfer, J. Yoo, A. Yamaguchi, E.C. Sanudo, T.R. Concolino, A.L. Rheingold, H. Ishimoto, D.N. Hendrickson, G. Christou, J. Am. Chem. Soc. 124 (2002) 9710;
(b) E.C. Sanudo, W. Wernsdorfer, K.A. Abboud, G. Christou, Inorg. Chem. 43 (2004) 4137;
(c) M. Soler, E. Rumberger, K. Folting, D.N. Hendrickson, G. Christou, Polyhedron 20 (2001) 1365.